Efficient Raman Lasing in Tapered Silicon Waveguides

The authors review the operating principles of a silicon Raman laser and show that by introducing a longitudinal variation of the waveguide width in the cavity, the lasing efficiency can be increased significantly.

Michael Krause, Hagen Renner, and Ernst Brinkmeyer

The recent demonstration of a continuous-wave silicon Raman laser (1) has been considered a major milestone in the expanding field of silicon photonics, which recently has witnessed significant progress in a lot of areas, including high-speed electro-optical modulators (2, 3) and sharp, low-loss waveguide bends (4). Such developments contribute to the continuing vision that a lot of optical functionality might one day be integrated tightly with electronic integrated circuits on silicon chips (5).

Among the various existing approaches to achieving light amplification and emission in silicon (6), the Raman effect is particularly attractive because it does not require any structural modification or introduction of dopants. Furthermore, it is applicable in the entire transparency range of silicon, provided that appropriate pump laser sources are available. Thus, technological processes that are standard in the electronics industry today can be used to build optical Raman amplifiers and lasers on a silicon chip. Since the first observation of stimulated Raman scattering in a silicon waveguide in 2003 (7), many groups have exploited this phenomenon to build chip-scale amplifiers (8–10) and wavelength converters (11), as well as pulsed (12) and continuous-wave (1) lasers.

Silicon Raman Laser

The Raman lasers considered here essentially consist of a silicon waveguide and reflectors for the Stokes (lasing) wavelength at the two ends of the waveguide, forming the laser cavity (see Figure 1). In the silicon-on-insulator (SOI) technology, silicon, with its high refractive index of about 3.5, forms the core of the waveguide (as shown in Figure 2). It is surrounded by materials of lower refractive index, typically a silica buffer layer below (refractive index of about 1.5), and silica or air above. The cavity reflectors can be formed by polished waveguide end surfaces, by thin-film coatings on the end surfaces, or by waveguide Bragg gratings. The Raman laser is pumped optically by a pump laser whose light is injected into the waveguide.

The operation principle of the laser is simple: when the pump laser at the wavelength λ_p is switched on, spontaneous Raman scattering will generate light at new wavelengths, the most intense peak being generated at the Stokes wavelength λ_s corresponding to an optical frequency downshifted by about 15.6 THz from the pump frequency. The spectral width of the Raman peak is about 100 GHz. Furthermore, any Stokes light in the cavity will be amplified through the effect of stimulated Raman scattering — it will experience Raman gain proportional to the amount of pump power. When reaching the ends of the waveguide, part of the Stokes light leaves the waveguide (forming the output beam), and part of it is reflected back into the waveguide. When the pump power is high enough, this feedback plus the amplification through stimulated Raman scattering leads to an increasing buildup of optical power at the Stokes wavelength. Eventually, a steady state is reached in which the laser continuously converts the pump radiation at λ_p to Stokes radiation at λ_s.

Nonlinear Absorption

However, there are two nonlinear absorption mechanisms that compete with the Raman gain and limit the efficiency of Raman lasing in silicon or even prevent it completely. First, even though silicon is transparent in the wavelength range of interest (λ = 1.1 . . . 5 μm), the effect of two-photon absorption (TPA) becomes noticeable at the high optical powers necessary for Raman amplification. In TPA, two photons are absorbed simultaneously, generating an electron-hole pair. The absorption caused by this effect alone does not impair the Raman-amplification process significantly. However, the increased conductivity of the silicon waveguide due to TPA-generated charge carriers leads in turn to additional optical losses called free-carrier absorption (FCA), which can indeed be substantial. The strength of FCA depends upon how much the carriers accumulate in the waveguide core before recombining. This is quantified by an effective charge-carrier lifetime τ_{eff}, which is lower when carriers quickly recombine or diffuse out of the areas of high light intensity.

The effective carrier lifetime τ_{eff} is a property of the waveguide determined by its geometry and the technological processes taken to manufacture it. If it is too high, it is impossible to make the waveguide lase. To reduce the lifetime and thus the impact of FCA, the authors in reference 1 applied a static electric field transversely across the waveguide. The field sucks the carriers out of the waveguide-core area after being generated by TPA before they can accumulate and cause significant FCA to the propagating light. The authors could indeed show that by increasing the applied electric field, the effective lifetime is decreased and lasing becomes more efficient.

On the other hand, we have recently proposed another way of increasing the efficiency of Raman amplification and lasing in silicon waveguides. By tapering — that is, varying the waveguide width along the propagation direction (as illustrated in Figure 1) — the balance between FCA and Raman gain can be adjusted optimally at each waveguide position and the net gain can be increased (13, 14). Before explaining this concept in detail, however, we have a look at the model for a standard Raman laser.

Raman-Laser Model

In our model for the steady-state characteristics of a silicon Raman laser, there are forward- (+) and backward-propagating (–) waves at the pump (p) and Stokes (s) wavelengths, the powers $P_{p,s}^{\pm}(z)$ of which change along the propagation direction $\pm z$ according to the differential equations (15) (see Figure 1).

$$\pm\frac{1}{P_p^{\pm}}\frac{dP_p^{\pm}}{dz} = -\alpha - \frac{g}{A_{eff}}\frac{\lambda_s}{\lambda_p}(P_s^{+} + P_s^{-}) - \frac{\beta}{A_{eff}}\left[P_p^{\pm} + 2\left(P_p^{\mp} + P_s^{+} + P_s^{-}\right)\right] - \tilde{\varphi}\lambda_p^2\tilde{N}_{eff}, \quad [1]$$

$$\pm\frac{1}{P_s^{\pm}}\frac{dP_s^{\pm}}{dz} = -\alpha + \frac{g}{A_{eff}}(P_p^{+} + P_p^{-}) - \frac{\beta}{A_{eff}}\left[P_s^{\pm} + 2\left(P_s^{\mp} + P_p^{+} + P_p^{-}\right)\right] - \tilde{\varphi}\lambda_s^2\tilde{N}_{eff}. \quad [2]$$

At each waveguide position z, the right-hand sides of Equations 1 and 2 represent the local gain for the pump and Stokes waves, respectively, which is the sum of four terms. The first term represents the linear losses α present in every optical waveguide, for example, due to light scattering at the waveguide-sidewall roughness produced during etching. The second term describes the effect of stimulated Raman scattering (it appears as a loss to the pump waves and as a gain to the Stokes waves) with a Raman-gain coefficient g. The third term describes TPA with the TPA coefficient β. Finally, the last term gives the loss due to FCA, which is proportional to an effective charge carrier density,

$$\tilde{N}_{eff}(z) = \frac{\beta\tau_{eff}}{2h\nu_p A_{eff}^2}\left\{P_p^{+2} + P_p^{-2} + P_s^{+2} + P_s^{-2} + 4\left[P_p^{+}P_p^{-} + P_s^{+}P_s^{-} + \left(P_p^{+} + P_p^{-}\right)\left(P_s^{+} + P_s^{-}\right)\right]\right\}, \quad [3]$$

where τ_{eff} is the effective carrier lifetime explained in the previous section. The expression for $\tilde{N}_{eff}$ is of second order in the optical powers, because carrier generation takes place through TPA as opposed to one-photon absorption. Note that spontaneous Raman scattering does not appear in our differential equations, as its contribution is negligible once the laser has reached its steady state.

An important constant appearing in Equations 1–3 is the effective area A_{eff}, which characterizes how strongly the waveguide confines the light. The efficiency of all nonlinear effects depends upon the intensity of light. Consequently, if the same optical power is confined to a smaller area A_{eff}, light intensity is higher and all nonlinear effects such as Raman scattering, TPA, and FCA are more effective (see Equations 1–3). Note in particular that the FCA term is inversely proportional to the square of A_{eff}.

Finally, the reflection of the Stokes (and, optionally, also the pump) waves at the two end faces of the SOI waveguide (at $z = 0$ and $z = L$) with the reflectivities $R_{\{p,s\},\{l,r\}}$ and the input coupling of the pump power P_0 are taken into account by the boundary conditions

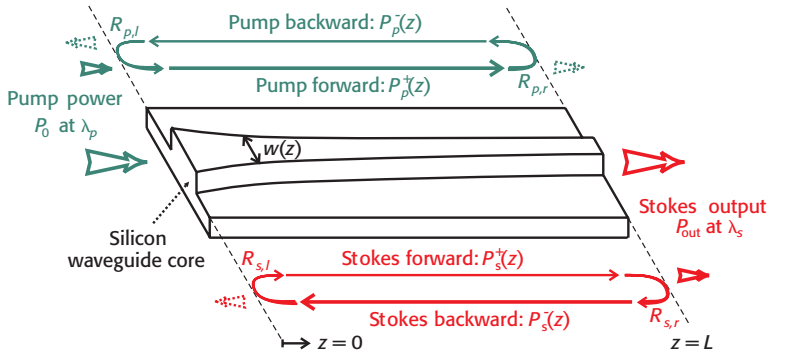

Figure 1. Schematic of a Raman laser in a tapered silicon-on-insulator rib waveguide. Note that in conventional silicon Raman lasers, the waveguide width $w(z)$ is constant.

$$P_p^+(0) = (1 - R_{p,l})P_0 + R_{p,l}P_p^-(0), \quad P_s^+(0) = R_{s,l}P_s^-(0), \qquad [4]$$

$$P_p^-(L) = R_{p,r}P_p^+(L), \qquad P_s^-(L) = R_{s,r}P_s^+(L). \qquad [5]$$

The right-hand output power of the laser is $P_{out} = P_s^+(L)(1 - R_{s,r})$.

In the boundary condition Equation 4a for pump-power injection, the injected and reflected powers simply add incoherently, because the pump-laser spectrum is so broad that it spans several free spectral ranges (FSRs) of the silicon-waveguide cavity. For example, the pump laser used in (7) is a Raman fiber laser with a spectral width of several tens of gigahertz, while a silicon-waveguide cavity with a length of 1 cm has an FSR of only $c/(2Ln) \approx 5$ GHz.

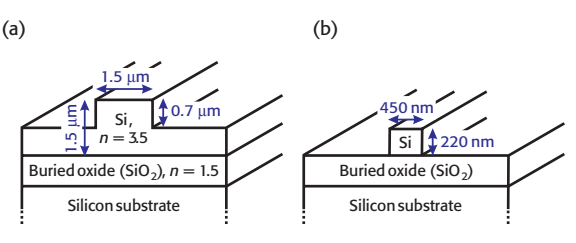

Figure 2. Two typical silicon-waveguide geometries. Left: rib waveguide as in (1). Right: strip waveguide as in (8).

Equations 1–5 have no known analytic solution and are solved numerically. Simulations presented in this article are performed for the same parameters as in (15): $g = 20$ cm/GW, $\alpha = 1.0$ dB/cm, $\beta = 0.7$ cm/GW, and an FCA efficiency of $\overline{\varphi} = 6.0 \times 10^{-10}$. The pump and Stokes wavelengths are $\lambda_p = 1427$ nm and $\lambda_s = 1542$ nm, respectively. We will consider only lasers that have been prepared such that they have a left-hand Stokes reflectivity of $R_{s,l} = 100\%$ (that is, we want to have all the laser output power on the right-hand side), whereas the other reflectivities have the reflectivity of a polished silicon–air interface of $R_{p,l} = R_{p,r} = R_{s,r} = 30\%$.

Optimal Nontapered Laser

The practical question arises: What is the maximum output power we can obtain from a standard, nontapered silicon Raman laser with the parameters given at the end of the previous section? We assume that the waveguide technology has led to an effective carrier lifetime of $\tau_{eff} = 4.5$ ns. Then the only remaining unspecified parameters are the effective area A_{eff} and the waveguide length L. In Figure 3, we vary these two parameters and plot the maximum output power of the resulting lasers, assuming that our pump laser is limited to 4W of power. The optimal laser, marked with a black asterisk in Figure 3, has an effective area of $A_{eff} = 2.96$ µm^2 and a length of $L = 45.6$ mm and gives 4.3 mW of output power at the maximum available pump power of 4 W. Figure 4 shows how the pump (green) and Stokes (red) powers are longitudinally distributed inside the cavity of the optimal laser. At the left-hand side of the cavity, the amplification of the Stokes light can be seen clearly; however, toward the right-hand side, the Raman gain becomes smaller as less pump power arrives there. At the right-hand waveguide end, about 6 mW of Stokes power (solid red) are incident, of which $R_{s,r} = 30\%$ are reflected, forming the backward-propagating Stokes wave (dashed red). The remaining 4.3 mW are transmitted and yield the laser output power.

The most interesting aspects of the laser are its characteristics — that is, the curve showing the output power in terms of the pump power. The characteristics of the optimal laser are shown as the thin solid line in Figure 5a. The laser starts operating at a pump power of 3.1 W. Beyond this lasing threshold, the output power increases initially when the pump power is increased. Eventually, however, there is a rollover at $P_0 = 4.2$ W and a decrease of the output power up to the shutdown threshold of 5.7 W, at

which laser operation breaks down (15). This effect is due to FCA loss, which ultimately increases faster (with the square of the pump power) than the Raman gain, which increases only linearly with the pump power (see Equations 1–3).

Note that if the effective area were made smaller than the optimal value, the result would be stronger FCA and less efficient lasing due to the dependence of FCA upon the square of $1/A_{\text{eff}}$ (see Equation 3). On the other hand, a larger effective area would lead to a strong reduction of FCA, but the Raman gain also would scale down as $1/A_{\text{eff}}$, so one is limited eventually by the available pump power. Consequently, there exists an optimum value for the effective area.

There also is an optimum waveguide length, because a waveguide that is too short would not provide enough interaction length for the Raman-amplification process. On the other hand, a waveguide that is too long would add an unnecessary amount of linear losses (characterized by α).

More output power could be obtained by using a waveguide with a shorter lifetime τ_{eff}, or by using a different set of mirror reflectivities. Instead of doing this, we will show next how a simple tapering of the waveguide — that is, a longitudinal variation of A_{eff} that can be realized by a waveguide-width variation (as illustrated in Figure 1) — can improve the characteristics by a factor of more than eight.

The Principle Behind Tapering

As discussed earlier, the onset of FCA at high pump powers limits the achievable laser efficiency. To motivate the concept of the waveguide taper, we have a closer look at Equation 2 describing the local Stokes gain at position z. Note that in the case of the optimal laser presented in the previous section, the Stokes powers are much smaller than the pump powers (see Figure 4). Furthermore, we consider for simplicity the related case in which the righthand pump reflector is $R_{p,r} = 0$, so that a backward-propagating pump wave is not present. This simplified situation corresponds to the case of a so-called undepleted single-pass Raman amplifier, where a very weak Stokes signal is amplified through stimulated Raman scattering by a strong pump signal, which is injected codirectionally (13). The Stokes gain (Equation 2) then can be written

$$\frac{1}{P_s^+}\frac{\mathrm{d}P_s^+}{\mathrm{d}z} = -\alpha + (g - 2\beta)\frac{P_p^+}{A_{\text{eff}}} - \frac{\bar{\varphi}\lambda_s^2\beta\tau_{\text{eff}}}{2h\nu}\frac{P_p^{+2}}{A_{\text{eff}}^2}. \qquad [6]$$

The three terms on the right-hand side of Equation 6 correspond to, respectively, linear waveguide losses, an effective Raman gain describing joint action of stimulated Raman gain and TPA loss, and FCA loss. The right-hand side should be as large as possible at each position z inside the amplifier or laser, in order to make the overall Stokes gain large and lasing most efficient.

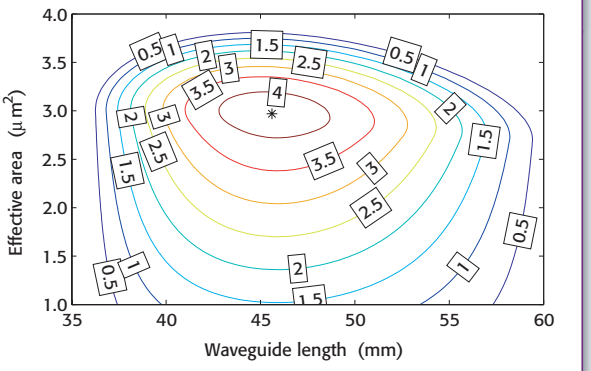

Figure 3. Contours of equal maximum output power in milliwatts for various silicon Raman lasers with nontapered effective area, when pump power is limited to 4 W.

It can be seen that the FCA term in Equation 6 dominates over the Raman-gain term at positions z inside the waveguide, where the pump power $P_p^+(z)$ is large, because the FCA term depends on the square of the pump power. However, the FCA term also inversely depends upon the square of the effective area A_{eff}, whereas the Raman-gain term depends inversely upon only the first power.

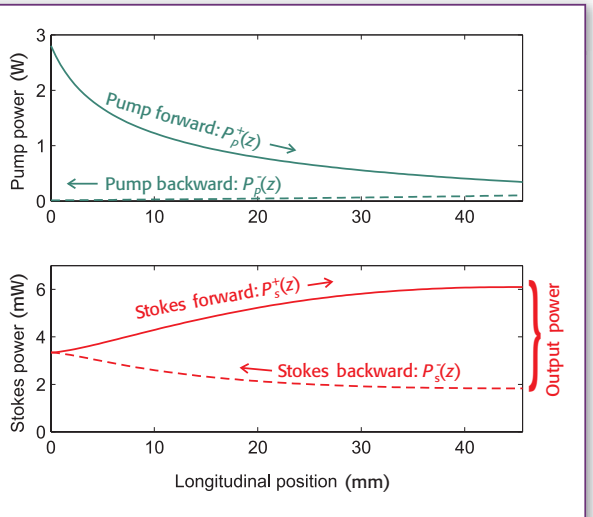

Figure 4. Longitudinal distribution of the powers of the waves propagating forward (solid) and backward (dashed) at the pump (green) and Stokes (red) wavelengths for the optimal non-tapered laser at a pump power of $P_0 = 4$ W.

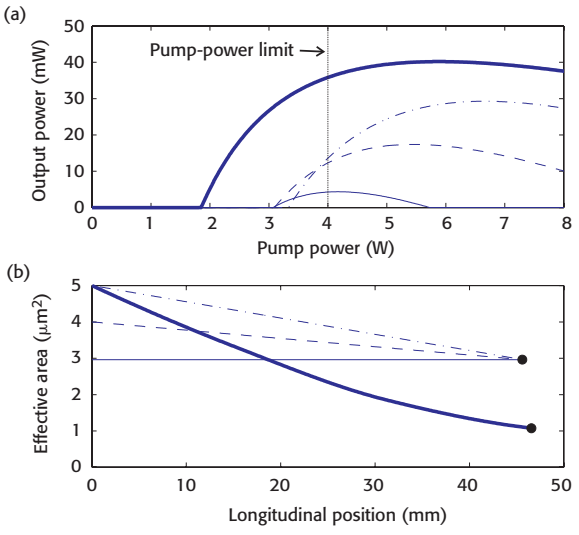

Figure 5. Comparison of several silicon Raman lasers: (a) characteristics (output power versus pump power) and (b) corresponding tapers (longitudinal variation of the effective area).

Tapered-Laser Characteristics

In this section, we will show that the effective-area taper can indeed improve the Raman-laser characteristics. Consider first the characteristics of the optimal nontapered laser found previously under the section "Optimal Nontapered Laser," plotted as the thin solid line in Figure 5a. The corresponding "taper" (constant effective area versus waveguide position) is plotted in Figure 5b. This laser yields 4.3 mW of output power at the maximum available pump power of 4W.

After the discussion in the previous section, we expect that increasing the effective area at the left-hand side of the waveguide improves the laser characteristics. The thin-dashed and dash-dotted curves in Figure 5 show two such arbitrarily chosen tapers and the corresponding laser characteristics. We did not chose any specially optimized tapers, yet both tapered lasers already produce more output power at $P_0 = 4$ W than the best nontapered laser. Finally, the thick solid curves in Figure 5 show the results for a laser for which we have optimized the taper $A_{\text{eff}}(z)$ (we have restricted the allowed effective area to the range $1 \ldots 5\ \mu\text{m}^2$) and the waveguide length L. The output power of this optimized tapered laser, 36 mW, is larger by a factor of more than eight than that of the best nontapered laser.

Consequently, by changing the value of A_{eff}, we can shift the relative weighting between the Raman-gain and FCA-loss terms — if FCA is too large because of large pump powers, we should increase A_{eff}. This would result in an undesired reduction of the Raman gain according to $1/A_{\text{eff}}$ but simultaneously in a much stronger reduction of the FCA-loss term according to $1/A^2_{\text{eff}}$. Consequently, if we allow the effective area to vary longitudinally, we should simply choose $A_{\text{eff}}(z)$ such that the right-hand side of Equation 6 is maximal at each waveguide position z; in other words, the balance between Raman gain and FCA is optimized at each z according to the local pump power $P_p^+(z)$.

The typical shape for a taper is a decrease of A_{eff} toward regions of lower pump power: the latter is injected at the left-hand side ($z = 0$) and decreases towards the right-hand side because it loses power to the Stokes waves in the Raman-amplification process (an example for the pump-power distribution is shown in Figure 4). Therefore, the optimal effective area typically will be larger at the pumped end of the waveguide and smaller at the opposite end. However, the optimal solution for $A_{\text{eff}}(z)$ is known in exact analytic form only for the case of an undepleted Raman amplifier, in which the result is that $A_{\text{eff}}(z)$ should have an exponentially decaying shape along z (13). For a Raman laser, a numerical optimization of the taper is necessary (14), for which we have employed a standard genetic algorithm (16).

Note that the factor of eight is only one specific example. If the lifetime τ_{eff} of our waveguide were larger than the value we have used here (4.5 ns), the efficiency improvement from the nontapered to the tapered laser would be even larger. The most dramatic effect is obtained when τ_{eff} is so large that there simply exists no nontapered laser, and only with a taper it is possible to make the waveguide lase (14).

Conclusion

We have reviewed the operation principles of a Raman laser in a silicon waveguide. The nonlinear effect of FCA competes with stimulated Raman gain and sets an upper limit to the achievable laser efficiency. We have shown that by varying the width of the waveguide longitudinally, the balance between FCA and Raman gain can be optimized at each position inside the cavity, and thus, Raman amplification can be more efficient than in constant-width waveguides. An example calculation has shown that such a waveguide taper leads to a lasing-efficiency increase by a factor of more than eight.

References

1. H. Rong, R. Jones, A. Liu, O. Cohen, D. Hak, A. Fang, and M. Paniccia, *Nature* **433**, 725–727 (2005).
2. L. Liao, D. Samara-Rubio, M. Morse, A. Liu, D. Hodge, D. Rubin, U.D. Keil, and T. Franck, *Opt. Express* **13**(8), 3129–3135 (2005).
3. Q. Xu, B. Schmidt, S. Pradhan, and M. Lipson, *Nature* **435**, 325–327 (2005).
4. Y.A. Vlasov and S.J. McNab, *Opt. Express* **12**(8) 1622–1631 (2004).
5. G.T. Reed, *Nature* **427**, 595–596 (2004).
6. L. Pavesi and D.J. Lockwood, Eds. *Silicon Photonics* (Springer-Verlag Berlin Heidelberg, 2004).
7. R. Claps, D. Dimitropoulos, V. Raghunathan, Y. Han, and B. Jalali, *Opt. Express* **11**(15), 1731–1739 (2003).
8. R.L. Espinola, J.I. Dadap, J. Richard M. Osgood, S.J. McNab, and Y.A. Vlasov, *Opt. Express* **12**(16), 3713–3718 (2004).
9. Q. Xu, V.R. Almeida, and M. Lipson, *Opt. Express* **12**(19), 4437–4442 (2004).
10. T.K. Liang and H.K. Tsang, *Appl. Phys. Lett.* **85**(16), 3343–3345 (2004).
11. V. Raghunathan, R. Claps, D. Dimitropoulos, and B. Jalali, *J. Lightwave Technol.* **23**(6), 2094–2102 (2005).
12. O. Boyraz and B. Jalali, *Opt. Express* **12**(21), 5269–5273 (2004).
13. H. Renner, M. Krause, and E. Brinkmeyer, "Maximal Gain and Optimal Taper Design for Raman Amplifiers in Silicon-on-Insulator Waveguides," in *Integrated Photonics Research and Applications Topical Meeting (IPRA)*, 2005, paper JWA3.
14. M. Krause, H. Renner, and E. Brinkmeyer, "Efficiency increase of siliconon-insulator Raman lasers by reduction of free-carrier absorption in tapered waveguides," in *Conference on Lasers and Electro-Optics (CLEO)*, 2005, paper CThB1.
15. M. Krause, H. Renner, and E. Brinkmeyer, *Opt. Express* **12**(23), 5703–5710 (2004).
16. J. Lampinen, *A Bibliography of Differential Evolution Algorithm*, Lappeenranta University of Technology, Department of Information Technology, Laboratory of Information Processing, 2001, available via Internet: http://www.lut.fi/ jlampine/debiblio.htm. ■

Michael Krause, Hagen Renner, and **Ernst Brinkmeyer** are with Technische Universität Hamburg-Harburg (Hamburg, Germany; http://www.om.tu-harburg.de). E-mail: m.krause@tu-harburg.de.